Physics of the Earth and Planetary Interiors 305 (2020) 106504

Contents lists available at ScienceDirect

Physics of the Earth and Planetary Interiors

journal homepage: www.elsevier.com/locate/pepi

Seismic anisotropy in the lowermost mantle beneath North America from SKS-SKKS splitting intensity discrepancies

Katherine A. Lutz[a,b,*], Maureen D. Long[b], Neala Creasy[b,c], Jie Deng[b,d]

[a] Department of Astronomy, Yale University, New Haven, CT 06520, United States of America
[b] Department of Geology and Geophysics, Yale University, New Haven, CT 06520, United States of America
[c] Now at: Department of Geophysics, Colorado School of Mines, Golden, CO 80401, United States of America
[d] Now at: Department of Earth, Planetary, and Space Sciences, University of California, Los Angeles, Los Angeles, CA 90095, United States of America

ABSTRACT

We examined SKS-SKKS splitting intensity discrepancies for phases that sample the lowermost mantle beneath North America, which has previously been shown to exhibit seismic anisotropy using other analysis techniques. We examined data from 25 long-running seismic stations, along with 244 stations of the temporary USArray Transportable Array, located in the eastern, southeastern and western U.S. We identified 279 high-quality SKS-SKKS wave pairs that yielded well-constrained splitting intensity measurements for both phases. Of the 279 pairs, a relatively small number (15) exhibited discrepancies in splitting intensity of 0.4 s or greater, suggesting a contribution to the splitting of one or both phases from anisotropy in the lowermost mantle. Because only a small minority of SK(K)S phases examined in this study show evidence of being affected by lowermost mantle anisotropy, the traditional interpretation that splitting of these phases primarily reflects anisotropy in the upper mantle directly beneath the stations is appropriate. The discrepant pairs exhibited a striking geographic trend, sampling the lowermost mantle beneath the southern U.S. and northern Mexico, while other regions were dominated by non-discrepant pairs. We carried out ray theoretical modeling of simple anisotropy scenarios that have previously been suggested for the lowermost mantle beneath North America, invoking the alignment of post-perovskite due to flow induced by the impingement of the remnant Farallon slab on the core-mantle boundary. We found that our measurements are generally consistent with this model and with the idea of slab-driven flow, but relatively small-scale lateral variations in the strength and/or geometry of lowermost mantle anisotropy beneath North America are also likely present.

1. Introduction

The D" layer, the lowermost 200–300 km of Earth's mantle, plays host to notable heterogeneity in seismic properties and likely in geochemical and/or compositional properties as well (e.g. Garnero and McNamara, 2008). The lowermost mantle represents a thermal boundary layer between the hotter core and the cooler mantle and exhibits properties that contrast with the bulk of the lower mantle above it. Examples of unusual geophysical properties include the presence of two large regions of relatively low shear wave velocities (Large Low Shear Velocity Provinces, or LLSVPs; Garnero et al., 2016; McNamara, 2019), localized regions of particularly low velocity (known as Ultra-Low Velocity Zones or ULVZs; Garnero et al., 1998; McNamara, 2019), and intermittently observed seismic discontinuities that likely correspond to the phase transition between bridgmanite and post-perovskite (e.g., Murakami et al., 2004; Hernlund et al., 2005). Another aspect of lowermost mantle structure that contrasts with the bulk of the lower mantle is the presence of seismic anisotropy, or directionally dependent seismic wave speeds (e.g., Vinnik et al., 1995; Garnero et al., 2004; Wang and Wen, 2007; Long, 2009; Nowacki et al., 2010, 2011; Cottaar and Romanowicz, 2013; Lynner and Long, 2014; Long and Lynner, 2015; Romanowicz and Wenk, 2017; Creasy et al., 2017; Grund and Ritter, 2018; Reiss et al., 2019; Wolf et al., 2019).

Seismic anisotropy is an important property because of the causative link between mantle deformation and the resulting anisotropy. When the mantle is deformed under dislocation creep (specifically via a dislocation glide mechanism; e.g., Cordier et al., 2012; Marquardt and Miyagi, 2015; Kraych et al., 2016), it forms a texture (often referred to as crystallographic preferred orientation, or CPO) that gives rise to seismic anisotropy at the macro scale. Measurements of seismic anisotropy can thus constrain the deformation geometry in various parts of the Earth, including the upper mantle (e.g., Karato et al., 2008; Becker et al., 2012; Long, 2013; Yuan and Beghein, 2014), the transition zone and uppermost lower mantle (e.g., Nowacki et al., 2015; Lynner and Long, 2015; Mohiuddin et al., 2015; Chang et al., 2016), and the lowermost mantle, which we investigate in this study. The characterization of seismic anisotropy at the base of the mantle has the potential to reveal patterns of flow and deformation just above the core-mantle boundary (CMB), informing our view of mantle dynamics in this crucial region (e.g., Nowacki et al., 2011).

* Corresponding author at: Department of Astronomy, Yale University, New Haven, CT 06520, United States of America.
E-mail address: katherine.lutz@aya.yale.edu (K.A. Lutz).

https://doi.org/10.1016/j.pepi.2020.106504
Received 28 January 2020; Received in revised form 6 May 2020; Accepted 11 May 2020
Available online 13 May 2020
0031-9201/

Seismic anisotropy in the lowermost mantle manifests itself in the seismic wavefield in several ways, including the splitting or birefringence of shear waves that propagate through the region. A variety of shear phases may be affected by anisotropy; common phases to study include ScS (e.g., Wookey et al., 2005a, 2005b; Nowacki et al., 2010; Ford et al., 2015; Creasy et al., 2017; Pisconti et al., 2019; Wolf et al., 2019) and SK(K)S phases (e.g., Niu and Perez, 2004; Restivo and Hellfrich, 2006; Wang and Wen, 2007; Long, 2009; He and Long, 2011; Lynner and Long, 2012, 2014; Roy et al., 2014; Deng et al., 2017; Reiss et al., 2019; Grund and Ritter, 2018; Asplet et al., 2020). A common strategy for the latter type of data is to measure splitting for SKS and SKKS phases recorded on the same seismogram (that is, SK(K)S phases from the same event-station pair). These phases sample the upper mantle in a nearly identical way, but diverge significantly in the lower mantle (Fig. 1); therefore, when significant discrepancies in measured splitting parameters for SKS vs. SKKS are identified, they are often interpreted as requiring a contribution to splitting from anisotropy at the base of the mantle to one or both phases.

Our work is motivated by two distinct goals. The first, and main, goal of the work presented here is to study seismic anisotropy at the base of the mantle beneath North America, which has previously been shown to be anisotropic (e.g., Panning and Romanowicz, 2006; Nowacki et al., 2010), using SK(K)S phases. While ScS splitting observations have already revealed lowermost mantle anisotropy beneath parts of North America (Nowacki et al., 2010), the geographical coverage of ScS phases beneath the continent is imperfect, and this coverage can be augmented by considering SK(K)S phases. Furthermore, recent modeling work (Ford et al., 2015; Creasy et al., 2017, 2019, 2020) has demonstrated that tighter constraints on anisotropic geometry can potentially be obtained by combining different types of observations (for example, ScS, SKS, and/or SKKS phases). Our second goal is to understand whether lowermost mantle anisotropy significantly contributes to the splitting of SK(K)S phases observed in eastern North America, which has recently been intensively studied (e.g., Long et al., 2010; Long et al., 2016; Wagner et al., 2012; White-Gaynor and Nyblade, 2016; Yang et al., 2017; Aragon et al., 2017; Li et al., 2019) and which is typically interpreted in terms of upper mantle processes (e.g., Becker et al., 2012). This question is important because the complex SKS splitting patterns beneath eastern North America are usually interpreted to reflect laterally and/or vertically heterogeneous anisotropy in the upper mantle. If, instead, some of this complexity is due to contributions from the lowermost mantle, then previous interpretations of SKS splitting beneath eastern North America may need to be revisited. Because of our interest in the second question, we began our study with a set of 15 permanent seismic stations in eastern North America, several of which were found by Long et al. (2010) to exhibit complex SKS splitting patterns. Specifically, a few of the stations examined by Long et al. (2010) exhibited strong, clear splitting over a set of narrow backazimuthal ranges, with clear null (that is, non-split) arrivals from a larger range of backazimuths. Because SKS splitting patterns such as these can reflect a localized contribution from lowermost mantle anisotropy (e.g., Lynner and Long, 2012), an outstanding question from the Long et al. (2010) study is whether anisotropy in the lowermost mantle may be contributing significantly to SKS splitting observations in eastern North America.

Based on initial observations of SKS-SKKS discrepancies at the permanent stations examined by Long et al. (2010), described below, we expanded our study to include additional stations in order to target a region of the lowermost mantle beneath the southern U.S. and northern Mexico (Fig. 2). We incorporated data from an additional 10 permanent stations and 244 temporary stations (mainly from the USArray Transportable Array, or TA), as shown in Fig. 2. We ultimately produced a data set of 279 of high-quality SKS-SKKS phase pairs, of which a relatively small number (15) exhibited significant discrepancies in splitting that cannot be easily explained in terms of upper mantle anisotropy models. We interpret these measurements as reflecting a contribution from anisotropy in the lowermost mantle to the splitting of one or both phases. In order to test whether our observations are consistent with previous studies of lowermost mantle anisotropy beneath North America based on ScS splitting (Nowacki et al., 2010), we carried out some simple forward modeling of elasticity scenarios proposed by Walker et al. (2011) for our study region. These models show that our measurements are generally consistent with deformation of post-perovskite in the lowermost mantle beneath North America, driven mainly by a large-scale downwelling associated with the impingement of a remnant of the Farallon slab on the CMB.

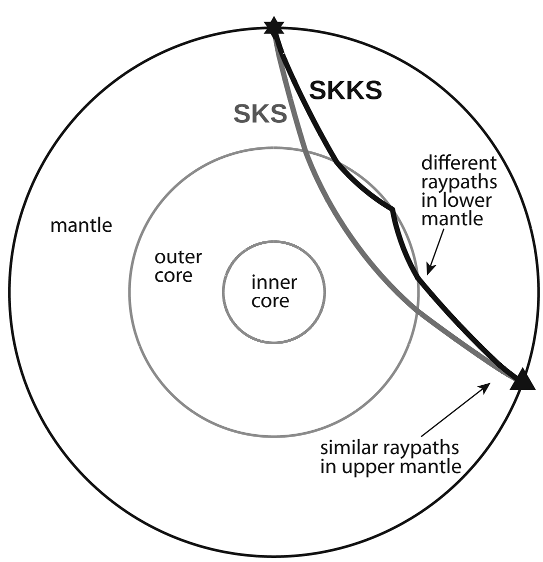

Fig. 1. Sketch of SKS (thick gray line) and SKKS (thick black line) seismic wave paths through the Earth at an epicentral distance relevant for our study. Raypaths from the source (star) to the receiver (triangle) were calculated for a shallow earthquake (event location at top of plot) using TauP (Crotwell et al., 1999) for the iasp91 Earth model (Kennett et al., 1995). Note the different paths for SKS and SKKS through the lowermost mantle, but similar paths in the upper mantle and transition zone on the receiver side, as indicated.

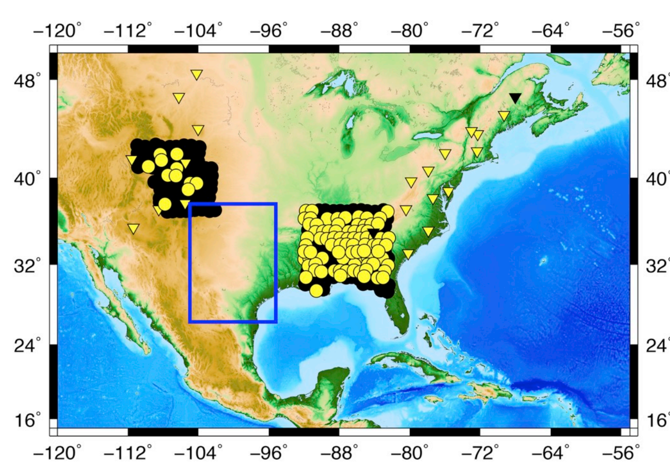

Fig. 2. Map of seismic stations used in analysis, including permanent stations of the U.S. national network and other networks (triangles), and temporary stations of the USArray Transportable Array (TA) stations (circles). Stations were chosen to target the region of the lowermost mantle shown with the blue rectangle. Stations which yielded high-quality SKS-SKKS pairs are shown in yellow, while stations for which data were examined but which did not yield high-quality SKS-SKKS pairs are shown in black. Background colors indicate topography/bathymetry. (For interpretation of the references to color in this figure legend, the reader is referred to the web version of this article.)

2. Data and methods

2.1. The SKS-SKKS splitting discrepancy method

This work relies on the SKS-SKKS splitting discrepancy method to identify seismic anisotropy in the lowermost mantle (e.g., Niu and Perez, 2004; Long, 2009; Lynner and Long, 2014; Roy et al., 2014; Long and Lynner, 2015; Deng et al., 2017; Grund and Ritter, 2018; Reiss et al., 2019; Wolf et al., 2019; Asplet et al., 2020). Shear wave splitting occurs when a shear wave propagates through an anisotropic medium (e.g., Silver and Chan, 1988; Vinnik et al., 1989). The shear wave is split into two quasi-S components, one fast and one slow; their polarization directions are controlled by the geometry of the anisotropy, and they accumulate a time delay as they travel through the medium at different speeds. The splitting of SKS and SKKS phases is commonly measured to probe upper mantle anisotropy, on the assumption that the lowermost mantle makes a negligible contribution to splitting in most cases (e.g., Niu and Perez, 2004; Long and Silver, 2009). In a small minority of cases, however, discrepancies between SKS and SKKS splitting for the same event-station pair suggest a contribution to splitting from lowermost mantle anisotropy to one or both phases. The inference of a lowermost mantle contribution is based on the raypath geometry involved (Fig. 1): SKS and SKKS rays have paths that are nearly identical in the upper mantle and mantle transition zone, but they diverge significantly at the base of the mantle, and they propagate through the lowermost mantle at significantly different propagation angles. This means that if there is anisotropy present, it will be sampled by the phases in a different way, due to their differences in propagation direction; furthermore, if there are lateral variations in anisotropy, then SKS and SKKS may sample different regions of anisotropic structure. Thus, any significant differences in splitting behavior between the two phases is often attributed to a contribution from the lowermost mantle (although some workers have argued that discrepant splitting may be interpreted solely in terms of upper mantle structure; e.g., Monteiller and Chevrot, 2010; Lin et al., 2014).

It is important to note that unless corrections for upper mantle anisotropy beneath the stations are explicitly applied (e.g., Lynner and Long, 2014; Lynner and Long, 2015; Ford et al., 2015), the SKS-SKKS discrepancy method cannot constrain the actual splitting parameters associated with the lowermost mantle portion of the raypath. Instead, discrepancies are typically taken to indicate a contribution to one or both phases from anisotropy at the base of the mantle. This could be a result of a lateral gradient in anisotropy at the base of the mantle, such that one phase is sampling anisotropy and the other is not, or such that both phases are sampling anisotropy, but with a different strength and/or geometry. Alternatively, anisotropy may be present at the base of the mantle in a geometry that would predict different splitting for SKS vs. SKKS phases because of their different (by about 15°) propagation directions (e.g., Tesoniero et al., 2020). Because there are several different possible explanations for SKS-SKKS splitting discrepancies, and because SK(K)S splitting measurements are often complicated by the presence of upper mantle anisotropy, their interpretation is not straightforward. This means that there are no simple rules of thumb for unambiguous inferences that may be made based on, for example, whether the SKS phase is more strongly split than the SKKS phase, or vice-versa. Despite these complications, however, strong SKS-SKKS splitting discrepancies are typically taken to indicate a contribution to splitting from lowermost mantle anisotropy from one or both phases, and therefore they serve as a useful complement to other methods for probing anisotropy at the base of the mantle (e.g., Creasy et al., 2019).

Another nuance in the interpretation of SKS-SKKS splitting discrepancies comes from the fact that while clearly discrepant splitting suggests a contribution from anisotropy in the lower mantle, it does not follow that an observation of non-discrepant splitting implies a lack of anisotropy at the base of the mantle (e.g., Long and Lynner, 2015). For any given non-discrepant SKS-SKKS pair, there are several possible scenarios that could explain the observation. The first, and most obvious, is a lack of lowermost mantle anisotropy. However, it is also possible that anisotropy is present at the base of the mantle but is contributing to the splitting of both SKS and SKKS phases in a similar way, and therefore no discrepancy between the two phases is evident. A third possibility is that there is anisotropy in the lowermost mantle, but the SK(K)S phases are propagating with a raypath geometry that does not cause splitting (that is, along the "null directions" of the anisotropy). It is therefore important to keep in mind, when interpreting maps of discrepant and non-discrepant SKS-SKKS pairs, that an observation of non-discrepant splitting does not necessarily imply a lack of lowermost mantle anisotropy in that region.

SKS-SKKS splitting discrepancies are often detected using conventional methods for measuring the shear wave splitting parameters ϕ (fast splitting orientation) and δt (delay time), such as the transverse component minimization method of Silver and Chan (1988) or the cross-correlation method of Ando et al. (1983) (e.g., Niu and Perez, 2004; Long, 2009; Lynner and Long, 2014; Long and Lynner, 2015). However, several recent studies have instead used measurements of the splitting intensity (Chevrot, 2000) to characterize SKS-SKKS splitting discrepancies, on the grounds that it is a more robust measurement for individual waveforms (Deng et al., 2017; Grund and Ritter, 2018; Reiss et al., 2019; Wolf et al., 2019; Asplet et al., 2020). This robustness comes at the expense of the additional information contained in estimates of the classical splitting parameters, however. In this study we measure both the traditional splitting parameters (ϕ, δt) and splitting intensity, and we rely on differences in splitting intensity values to characterize discrepancies.

2.2. Data and measurement strategy

We initially focused on measuring SKS-SKKS wave pairs for 15 long-running or permanent seismic stations in eastern North America. These stations are part of the United States National Seismic Network (station code: US), New England Seismic Network (station code: NE), Global Seismograph Network (station code: IU), or the Lamont-Doherty Cooperative Seismographic Network (station code: LD). Known issues with the alignment of horizontal components were corrected at stations GOGA, SSPA, and TZTN. At two of the 15 permanent stations, we examined data but did not identify any robust SKS-SKKS pairs. After our initial analysis identified evidence for discrepant SKS-SKKS pairs for waves that sampled the lowermost mantle beneath the south-central U.S. and northern Mexico (blue rectangle in Fig. 2), we expanded the set of stations used to include 156 stations of the USArray Transportable Array in the southeastern U.S. These stations were chosen because SK(K)S phases recorded from earthquakes originating in the western Pacific sample the region of interest in the lowermost mantle (Fig. 2). Finally, in order to obtain crossing paths that sample our study region in the lowermost mantle, we examined data from 98 stations (10 permanent, 88 temporary) located in and around the U.S. state of Colorado (Fig. 2). SK(K)S phases from earthquakes originating in the Scotia Arc and measured at these stations also sample our region of interest. A complete list of stations used in this study can be found in Supplementary Table S1.

Data for these stations were obtained from the Data Management Center (DMC) of the Incorporated Research Institutions for Seismology (IRIS). We examined data for earthquakes with moment magnitudes of 6.5 and greater at epicentral distances between 108°-122°, as both SKS and SKKS phases are typically visible in this range (e.g., Reiss et al., 2019). The events used in this study mainly originated in the western Pacific subduction zones or in the Scotia subduction zone, with a few events from the India-Eurasia collision zone and a few events elsewhere (Fig. 3). We bandpass filtered all waveforms to retain energy at periods between 8 (or 10) s and 25 s, with the lower period bound manually selected to optimize the clarity of each waveform. Our choice of bandpass filter was motivated by the desire to use a similar filter as that

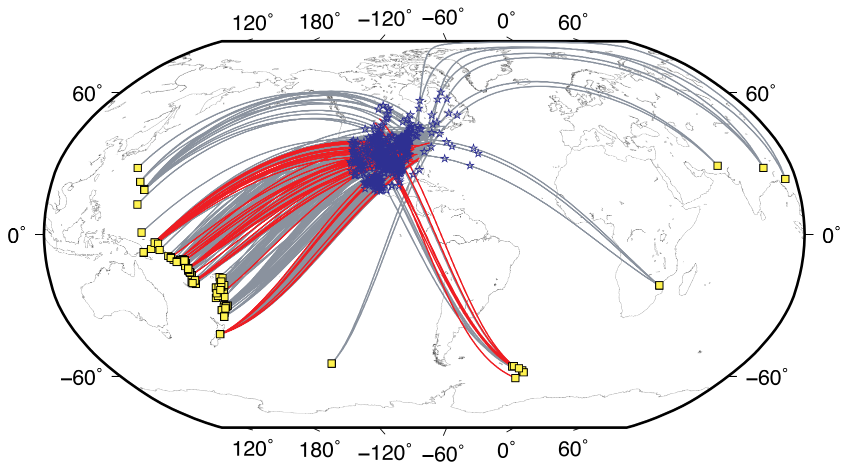

Fig. 3. Map of earthquakes and lowermost mantle pierce points for SKS-SKKS pairs presented in this study. Locations of all earthquakes that yielded at least one usable SKS-SKKS pair are shown with yellow squares; lines indicate the great circle path for each SKS-SKKS pair. Paths that exhibit some degree of discrepant SKS-SKKS splitting intensities are shown in red, while other paths are shown in gray. Blue stars show the pierce points at a depth of 2700 km for the SKS and SKKS phases. (For interpretation of the references to color in this figure legend, the reader is referred to the web version of this article.)

used in previous work on SK(K)S splitting in eastern North America (Long et al., 2010, 2016; Wagner et al., 2012), because on one of our goals is to understand to what extent lowermost mantle anisotropy might contribute to SK(K)S splitting datasets. We note that adjusting the high-frequency cutoff to a lower period range would make it easier for us to characterize splitting with low delay times (e.g., Walpole et al., 2014); however, this would come at the cost of including more noise in the microseism period band in the waveforms, and would allow for a less straightforward comparison to previous work.

We followed the shear wave splitting measurement methodology used by Deng et al. (2017), using a modified version of the SplitLab software (Wüstefeld et al., 2008) that measures splitting intensity (SI) using the method described in Chevrot (2000). The splitting intensity corresponds to the amplitude ratio between the transverse component energy and the time derivative of the radial component energy (Chevrot, 2000). It is related to the splitting parameters (ϕ, δt) via the approximate relation $SI = -\frac{1}{2}\delta t \sin 2\beta$, where β is the angle between the backazimuth and the fast polarization direction ϕ. (We note that there are differences in the literature as to whether the splitting intensity quantity is defined with the factor of $\frac{1}{2}$, as above, or without it; this issue is discussed in some detail in Deng et al. (2017). As long as there is consistency in relating SI to the corresponding splitting parameters, then either formulation is acceptable.) Strongly split waves will have SI values with large absolute values, while waves that are not split (that is, null arrivals), or are only weakly split, will have SI values that are close to zero. We processed the data (approximately 5000 records in total) to identify seismograms with high-quality SKS and SKKS arrivals and measured both the traditional splitting parameters and the splitting intensity values, with error estimates, for each phase. For our estimates of (ϕ, δt), we relied on the rotation-correlation method of Bowman and Ando et al. (1983), as implemented in the SplitLab code (Wüstefeld et al., 2008). For both the SI and the rotation-correlation methods, we manually windowed each phase for analysis, choosing a window that began a few sections before the visually picked onset of SK(K)S energy and covered at least one full period of the signal (average window length was ~20 s), and visually checked the quality of each measurement.

3. Results

Our final set of SKS-SKKS splitting discrepancy measurements consisted of 279 high-quality SKS-SKKS pairs measured at 173 different seismic stations (Supplementary Table S2). We define as "high-quality" those pairs that meet the following criteria: 1) both SKS and SKKS phases were clearly visible, with good waveform clarity and acceptable signal-to-noise ratio (SNR greater than approximately 3 on the radial component), 2) both phases had a well-constrained SI measurement, with error bars less than approximately ± 0.4 s, and 3) for phases with transverse component energy above the noise, we checked to ensure that the waveform shape was similar to the time derivative of the radial component, as predicted (Chevrot, 2000). We did not require that both phases have well-constrained estimates for the traditional splitting parameters, as we relied primarily on splitting intensity estimates to characterize discrepancies, as discussed below. The geographic sampling of the 279 high-quality phase pairs is shown in Fig. 3, which maps the great circle paths connecting sources to receivers for all pairs (both discrepant and non-discrepant), along with the pierce points at a depth of 2700 km in the lowermost mantle (just above the core-mantle boundary) for each phase (calculated using the TauP utility; Crotwell et al., 1999). Our data set samples the lowermost mantle beneath the central portion of North America well, with most phases propagating along a generally west-to-east path.

Of the 279 SKS-SKKS pairs identified in our study, 116 of these exhibited differences in the splitting intensity values measured for SKS and SKKS that were larger than the error bars on the measurements (that is, the 95% confidence regions for the splitting intensity measurements did not overlap). However, as discussed further in Section 4.1, only strongly discrepant SKS-SKKS pairs can reliably be interpreted as requiring a contribution from lowermost mantle anisotropy. Following previous work (Deng et al., 2017; Reiss et al., 2019), we labeled as "strongly discrepant" those phase pairs for which the difference in estimated splitting intensity was > 0.4 s. Of the 116 pairs that exhibited some discrepancies between SKS and SKKS splitting behavior, 15 of them were strongly discrepant. Typical waveform examples for a strongly discrepant pair, a weakly discrepant pair, and a non-discrepant pair are shown in Fig. 4. In the strongly discrepant splitting example, the SKS phase is clearly split (SI = −0.74 s) while the SKKS phase is nearly null (SI = −0.10 s). In the weakly discrepant example, both phases are split, but the SI values are (statistically) significantly different (SI = −0.54 s for SKS and SI = −0.80 s for SKKS). In the non-discrepant example, both phases are null, with SI values close to zero (SI = −0.05 s for SKS and SI = 0.02 s for SKKS).

We investigated the spatial relationships between the geographic sampling of our SKS-SKKS data and isotropic velocity structure at the base of the mantle. Fig. 5 shows the shear velocity structure at the base of the mantle from the GyPSuM tomography model (Simmons et al., 2010), along with pierce points at a depth of 2700 km for all SKS and SKKS phases in our dataset. Because our lowermost mantle anisotropy interpretation ultimately focuses on the strongly discrepant pairs, these pairs are highlighted on Fig. 5. Strikingly, the 15 strongly discrepant pairs in our dataset delineate a region of the lowermost mantle beneath the southern U.S. and northern Mexico, geographically coincident with a portion of a fast anomaly that is thought to represent a fragment of the Farallon slab just above the CMB (Nowacki et al., 2010). Interestingly,

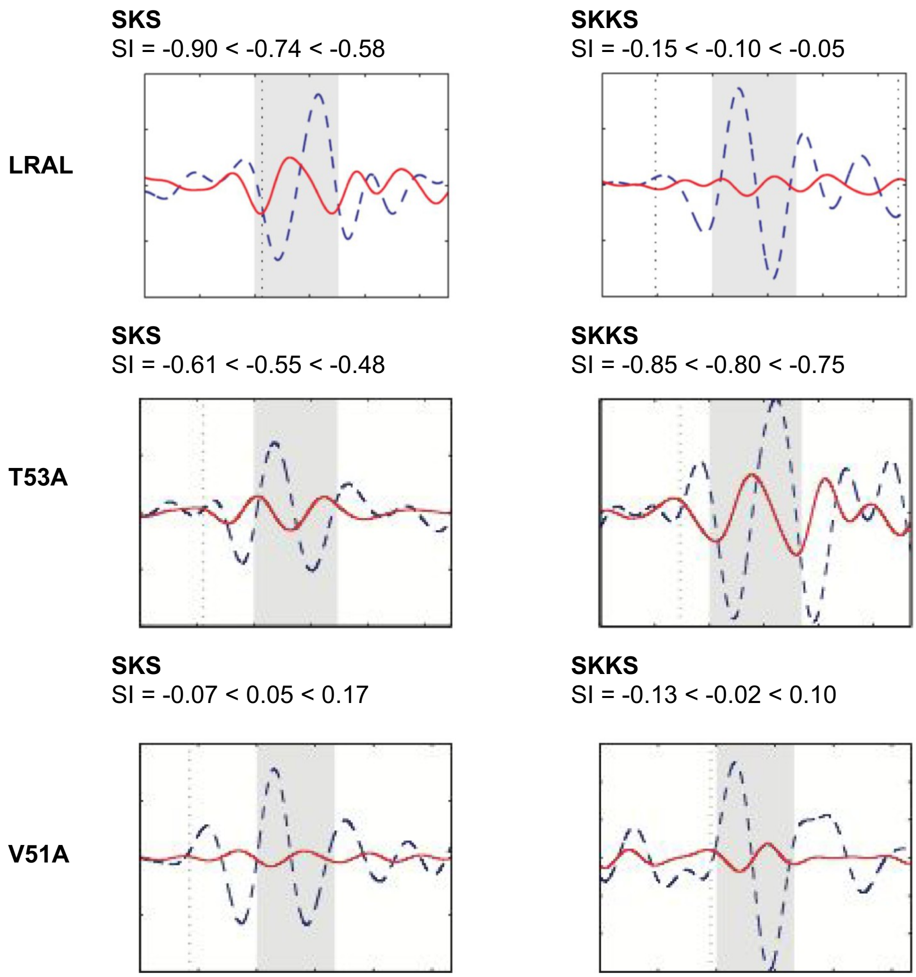

Fig. 4. Example SKS and SKKS waveforms from station LRAL (top), T53A (middle), and V51A (bottom). Left panels show SKS phases and right panels show the corresponding SKKS phases. Dashed blue lines show radial component waveforms and solid red lines show transverse component waveforms. Gray shading represents the time window used in each splitting intensity measurement. The measured splitting intensity value, along with the 95% confidence region, is shown above each panel. The top example shows a strongly discrepant SKS-SKKS pair (difference in splitting intensity of ~0.6 s), the middle example shows a weakly discrepant pair (difference in splitting intensity of ~0.2 s), and the bottom example shows a non-discrepant pair (difference in splitting intensity is negligible, and confidence regions for the two measurements overlap). (For interpretation of the references to color in this figure legend, the reader is referred to the web version of this article.)

however, there are many SKS-SKKS phases that do not exhibit strong discrepancies that also sample this fast anomaly, particularly to the north and east of the region with the discrepant pairs. It is also striking that in the region sampled by the discrepant pairs, there is a mix of discrepant and non-discrepant pairs that sample the same region of the mantle, behavior that is consistent with other studies of SKS-SKKS splitting discrepancies and lowermost mantle anisotropy (e.g., Long, 2009; Deng et al., 2017; Reiss et al., 2019).

4. Interpretation of SKS-SKKS splitting discrepancies

4.1. Upper mantle contributions: possible effects

The interpretation of SKS-SKKS splitting discrepancies must be done with great care (e.g., Monteiller and Chevrot, 2010; Tesoniero et al., 2020), for several reasons. SKKS has a longer raypath (and different ray parameter) through the lowermost mantle compared to SKS, and this may complicate the waveform behavior. Scattering from isotropic and/or anisotropic structures may affect the polarization of SK(K)S waves; in the presence of anisotropic structure, this effect may contribute to SKS-SKKS splitting discrepancies (Restivo and Helffrich, 2006), although scattering from purely isotropic structure is unlikely to perfectly mimic the waveform effects expected for shear wave splitting (e.g., Long and Lynner, 2015). Another complication is that any potential upper mantle effects must be accounted for before anisotropy in the lowermost mantle can reasonably be invoked.

Here we reiterate a line of reasoning from Reiss et al. (2019) that built on arguments in earlier papers (Long, 2009; Lynner and Long, 2014; Deng et al., 2017) about the relative contributions of the upper vs. lowermost mantle to SKS-SKKS discrepancies. As noted by Reiss et al. (2019) and elsewhere, it is well established that upper mantle anisotropy generally makes the first-order contribution to SK(K)S splitting on a global scale, while contributions from the lowermost mantle are at most a minor effect (e.g., Niu and Perez, 2004; Becker et al., 2012). Some studies have argued that SKS-SKKS splitting discrepancies can explained mainly in terms of upper mantle anisotropy (e.g., Monteiller and Chevrot, 2010; Lin et al., 2014). However, other papers (e.g., Long, 2009; Roy et al., 2014; Lynner and Long, 2014; Long and Lynner, 2015; Deng et al., 2017; Reiss et al., 2019; Grund and Ritter, 2018; Asplet et al., 2020) have argued that while anisotropy in the crust, upper mantle, or mantle transition zone may make a minor contribution to SKS-SKKS splitting discrepancies (due to small-scale lateral variations in anisotropic structure and/or to slight differences in ray propagation direction between the phases), these effects are likely to be relatively small. Specifically, unrealistically strong anisotropy in the crust or shallowest mantle is needed to generate significant discrepancies between SKS and SKKS phases; similarly, anisotropy in the mantle transition zone must be unrealistically strong as well as heterogeneous on very short length scales in order to generate observable discrepancies. Finite-frequency wavefield effects may contribute to differences in SKS and SKKS splitting even for simple, homogeneous upper mantle anisotropy models (e.g., Lin et al., 2014; Tesoniero et al., 2020); again, however, these effects are generally small (up to ~0.2 s difference in splitting intensity; see discussions in Long and Lynner, 2015 and Tesoniero et al., 2020). Therefore, while we acknowledge that anisotropy in the crust, upper mantle, and/or mantle transition zone may contribute to slight discrepancies in SKS-SKKS splitting (and thus to many of the discrepant paths shown in Fig. 3), we follow arguments

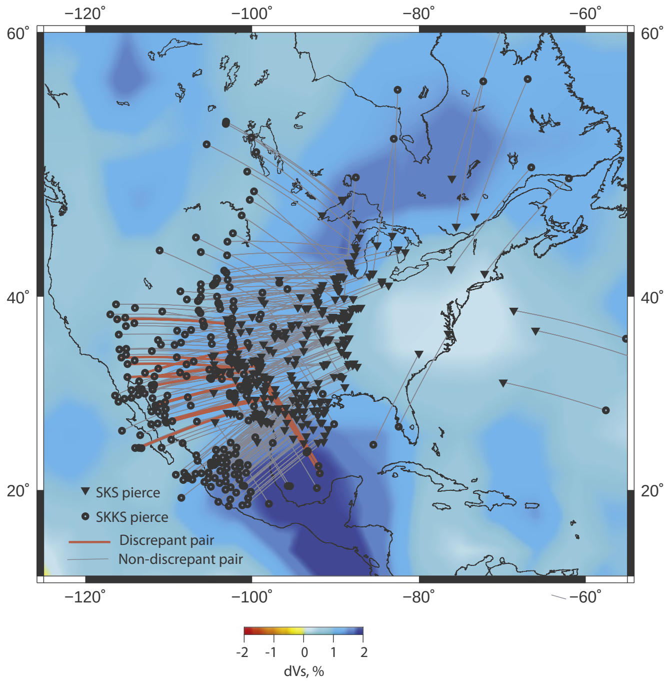

Fig. 5. Geographic sampling of the lowermost mantle for recorded SKS-SKKS pairs from all stations. SKS pierce points at a depth of 2700 km are shown with triangles and corresponding SKKS pierce points are shown with circles; gray or red lines connect pairs of phases, as shown by the legend. Red lines show strongly discrepant pairs; gray lines show other pairs (weakly discrepant or non-discrepant). Background colors show shear velocities at the base of the mantle (deviations from the background) from the GyPSuM tomography model (Simmons et al., 2010), with the color bar shown at the bottom (dVs values in %). Discrepant SKS-SKKS pairs in our study tend to sample near a fast anomaly at the base of the mantle, though to correspond to a remnant of the Farallon slab at depth (e.g., Nowacki et al., 2010). (For interpretation of the references to color in this figure legend, the reader is referred to the web version of this article.)

made in previous papers and interpret robust, strong discrepancies between SKS-SKKS splitting intensity (> 0.4 s; Fig. 5) as suggesting a contribution from the lowermost mantle.

One of the goals of this study was to understand whether lowermost mantle anisotropy might be a factor in explaining the complex splitting patterns observed at some permanent stations in eastern North America (Long et al., 2010), or whether, conversely, complex SK(K)S splitting in eastern North America mainly reflects upper mantle anisotropy. Our study identified strongly discrepant splitting in 15 out of 279 pairs (~5.4%), comparable to the fraction of discrepant pairs identified in the global study of Niu and Perez (2004). In our study, an observable contribution to SK(K)S splitting was identified for only a small set of raypaths, confined to certain azimuthal ranges, and associated with a specific region of the lowermost mantle. Therefore, we infer that, while the small minority of discrepant SKS-SKKS pairs can be used to characterize lowermost mantle anisotropy beneath North America, anisotropy at the base of the mantle is highly unlikely to make a first-order contribution to SK(K)S splitting patterns observed at stations in our study region. More specifically, an examination of the complex splitting patterns at long-running stations in eastern North America by Long et al. (2010) shows that at several stations, a mix of null and non-null arrivals are observed; with one exception (TZTN), each has non-null observations arriving from several distinct backazimuths. Because the discrepant SKS-SKKS pairs observed at eastern North American stations in this study arrive from a very narrow range of backazimuths, it is unlikely that anisotropy in the lowermost mantle exerts the primary control on patterns, although it may make a contribution to them in a few cases. In particular, station LRAL exhibited three discrepant SKS-SKKS pairs in our study, implying there is a contribution to splitting from the lowermost mantle at the relevant backazimuth. Furthermore, a detailed study of SKS splitting beneath the central Appalachian Mountains (Aragon et al., 2017) showed that many stations exhibit similar splitting parameters over a range of backazimuths, and that the splitting patterns could be reproduced well with models that invoked two layers of anisotropy in the upper mantle. Therefore, we conclude that SKS splitting measured in eastern North America (e.g., Long et al., 2010; Yang et al., 2017; Aragon et al., 2017; Li et al., 2019) likely primarily reflect anisotropy in the upper mantle, perhaps with some small and localized contribution from the crust and/or lowermost mantle in some places. There is no evidence from the SKS-SKKS data set presented here that contamination of SK(K)S phases observed in eastern North America from lowermost mantle anisotropy is pervasive.

4.2. *Lowermost mantle anisotropy inferred from splitting intensity discrepancies*

Proceeding with the line of reasoning articulated in Section 4.1, we interpret the large (> 0.4 s) discrepancies in splitting intensity we identified for 15 event-station pairs as reflecting a contribution from lowermost mantle anisotropy to one or both phases. Fig. 6 shows the geographic sampling of the lowermost mantle for these 15 pairs, along

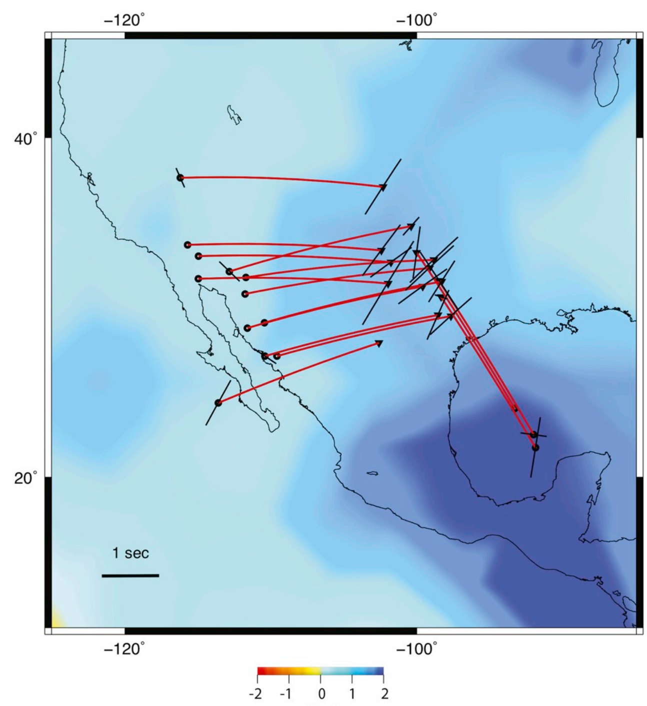

Fig. 6. Measured shear wave splitting parameters for strongly discrepant SKS-SKKS wave pairs identified in this study. SKS pierce points (at a depth of 2700 km) are shown with triangles and SKKS pierce points are shown with circles, with red lines connecting the pierce points for individual pairs, as in Fig. 5. Measured splitting parameters for individual phases are plotted at the pierce point as a black bar, with the orientation of the bar showing the fast splitting direction and the length of the bar indicating the splitting delay time, as shown by the scale bar at lower left. If no bar is plotted, then the splitting measurement was considered to be null. Note that splitting measurements have not been corrected for the effect of upper mantle anisotropy. Background colors show shear velocities at the base of the mantle (deviations from the background) from the GyPSuM tomography model (Simmons et al., 2010), with the color bar shown at the bottom (dVs values in %). (For interpretation of the references to color in this figure legend, the reader is referred to the web version of this article.)

with isotropic shear velocity structure from Simmons et al. (2010). Although these pairs were identified based on discrepancies in measured splitting intensity values (0.4 s or greater), we also plot on Fig. 6 the measured splitting parameters (ϕ, δt) for each phase, derived from the rotation-correlation method. We caution, however, that these splitting parameters cannot be interpreted simply as the contribution to splitting from lowermost mantle anisotropy, as discussed further below. The region of the lowermost mantle sampled by the discrepant pairs (Fig. 6) is located along a fast velocity anomaly that trends roughly north-south in this region and continues to the northeast (beneath the Hudson Bay region of Canada; see Fig. 5). This fast anomaly, which is also present in other tomographic models, is typically interpreted as a fragment of the subducted Farallon slab (e.g., Simmons et al., 2010; Nowacki et al., 2010). As Fig. 6 shows, the anomalous region of lowermost mantle anisotropy that we identify in this study is sampled both by discrepant pairs that have nearly west-to-east propagation paths and by discrepant pairs that have more nearly north-south propagation paths, with the latter group sampling near the SKS pierce points for the former group. Elsewhere beneath North America (Fig. 5), we do not observe discrepant pairs; again, this suggests that there is an anomalous region of lowermost mantle anisotropy beneath the central and southern U.S. and northern Mexico that is different from the surrounding mantle, either in terms of the presence, strength, or geometry of anisotropy.

Our identification of an anomalous region of lowermost mantle anisotropy beneath central North America comes with some caveats. As is common in studies of SKS-SKKS splitting discrepancies (e.g., Long, 2009; Lynner and Long, 2014; Deng et al., 2017; Reiss et al., 2019; Asplet et al., 2020), the anomalous region is sampled by a mix of discrepant and non-discrepant pairs. This behavior has been noted in many other studies; for example, Deng et al. (2017) identified a region of lowermost mantle anisotropy at the edge of the Pacific Large Low Shear Velocity Province (LLSVP) that was sampled by a mix of discrepant and non-discrepant SKKS pairs. Deng et al. (2017) showed that when individual SKS and SKKS waveforms from both discrepant and non-discrepant pairs were stacked, a discrepancy between SKS and SKKS splitting was evident in the stacked waveforms. (Unfortunately, in our study, the earthquakes associated with each of the relevant raypaths (west-to-east and south-to-north propagation) were not similar enough to successfully carry out the stacking technique of Deng et al. (2017)). Our observation of a mix of both discrepant and non-discrepant SKS-SKKS pairs, similar to the findings of previous studies, provides support for the idea that in the presence of realistic, complex Earth structure and for actual, noisy waveforms, a region of seismic anisotropy in the lowermost mantle can manifest itself as a mix of discrepant and non-discrepant individual SKS-SKKS pairs. Specifically, this behavior may be due to small-scale variations in anisotropic structure at the base of the mantle, to natural variability in noisy seismic data, or to technical limitations in the definition of discrepant SKS-SKKS pairs (Asplet et al., 2020). It may also reflect variability in the actual propagation direction for different SKS-SKKS pairs that have nominally similar raypaths. In a simple, 1-D Earth, phases that have similar raypaths (that is, similar backazimuths and ray parameters) will sample adjacent regions of the Earth's interior. If realistic 3-D velocity heterogeneity is present, however, then the rays may deviate from the great circle path due to refraction, and phases with similar backazimuths may actually be sampling different structure. The pierce points shown in Fig. 5 are calculated with a 1-D Earth model and therefore do not take into account this possible effect. Finally, it is worth keeping in mind that many of the pairs that were characterized as non-discrepant according to our cutoff (a difference of at least 0.4 s in splitting intensity estimates between SKS and SKKS) may, in fact, exhibit discrepancies of a smaller magnitude.

Another important caveat to our work is the fact that an observation of a non-discrepant pair (as pervasively identified beneath much of North America; Fig. 5) does not necessarily imply isotropic structure there. As discussed extensively by Long and Lynner (2015), a non-discrepant SKS-SKKS pair can be interpreted as reflecting one of three conditions: 1) the lowermost mantle being sampled is isotropic; 2) the lowermost mantle is anisotropic, but SKS and SKKS phases are experiencing the same shear wave splitting due to this anisotropy, or 3) the lowermost mantle is anisotropic, but the SKS and SKKS phases are polarized along a fast or slow splitting direction for the anisotropic medium, and thus both phases experience null splitting due to the anisotropy. We emphasize, therefore, that while the dominantly non-discrepant SKS-SKKS splitting behavior observed beneath much of North America is suggestive of a lack of strong or regionally coherent anisotropy (at least having a strength or geometry that causes significant splitting of SK(K)S phases), any individual non-discrepant pair cannot be interpreted as implying lower mantle isotropy.

Finally, we emphasize that because we did not explicitly correct for the effect of upper mantle anisotropy in our study, we cannot interpret the measurements in Fig. 6 as directly reflecting shear wave splitting due to lowermost mantle anisotropy. In order to isolate the effect of lowermost mantle anisotropy on SK(K)S splitting, it is necessary to accurately remove the contribution to splitting from the upper mantle. This correction can be done in cases where the upper mantle anisotropy beneath the stations is simple, with splitting patterns that reflect either a single homogeneous layer of anisotropy or that reflect little or no splitting due to the upper mantle (e.g., Lynner and Long, 2014; Long and Lynner, 2015). In order to confidently assess the character of upper mantle splitting patterns, however, long-running seismic stations with good backazimuthal coverage are needed. Stations with complex splitting patterns due to complicated anisotropic structure in the upper mantle (such as many of the stations examined by Long et al., 2010) or stations that have short deployment times (such as the TA stations that represent the bulk of receivers used in this study) are not good candidates for upper mantle anisotropy corrections. Therefore, the SKS-SKKS discrepancy measurements presented here can be interpreted as requiring a contribution to splitting from lowermost mantle anisotropy from one or both phases but cannot be directly interpreted to infer the geometry or strength of the responsible anisotropy. Despite this limitation, however, forward modeling can be carried out to test whether particular anisotropic scenarios are consistent with the data, as shown by previous studies (e.g., Reiss et al., 2019) and discussed further below.

We document three types of discrepant SKS-SKKS pairs in this study (Fig. 6). The most common is the case in which the SKS phase is split, but the SKKS phase is null (the majority of the pairs propagating along the west-to-east path in Fig. 6, and one pair along the south-to-north path). We also observe one pair in which SKS is null and SKKS is split (southernmost pair in the west-to-east group in Fig. 6) and several pairs (in both groups) in which both phases are split, but the splitting parameters are different. Because we did not explicitly correct for upper mantle contributions in our study, we cannot make any straightforward inferences about anisotropic structure based solely on the character of our discrepant results. This is because a null measurement for any given phase can either imply that the phase has not been split, or it can imply that it has been split by both upper and lowermost mantle anisotropy, with destructive interference of the splitting accrued in each layer. The dominance in our data set of pairs in which SKS is split but SKKS is null is an interesting observation, and somewhat counterintuitive, as SKKS phases have a longer path length through the lowermost mantle (due to their shallower propagation angle) and thus may in theory accrue a larger delay time in the presence of anisotropy. Again, however, the interpretation of this observation is not straightforward; one possibility is that anisotropy is present in the lower mantle in a geometry that leads to a different set of apparent splitting parameters for SKS vs. SKKS phases due to the difference in propagation angle. For example, Tesoniero et al. (2020) documented strong predicted discrepancies between SKS and SKKS splitting intensities for a lowermost mantle anisotropy model based on post-perovskite, due to the differences in propagation direction between the two phases.

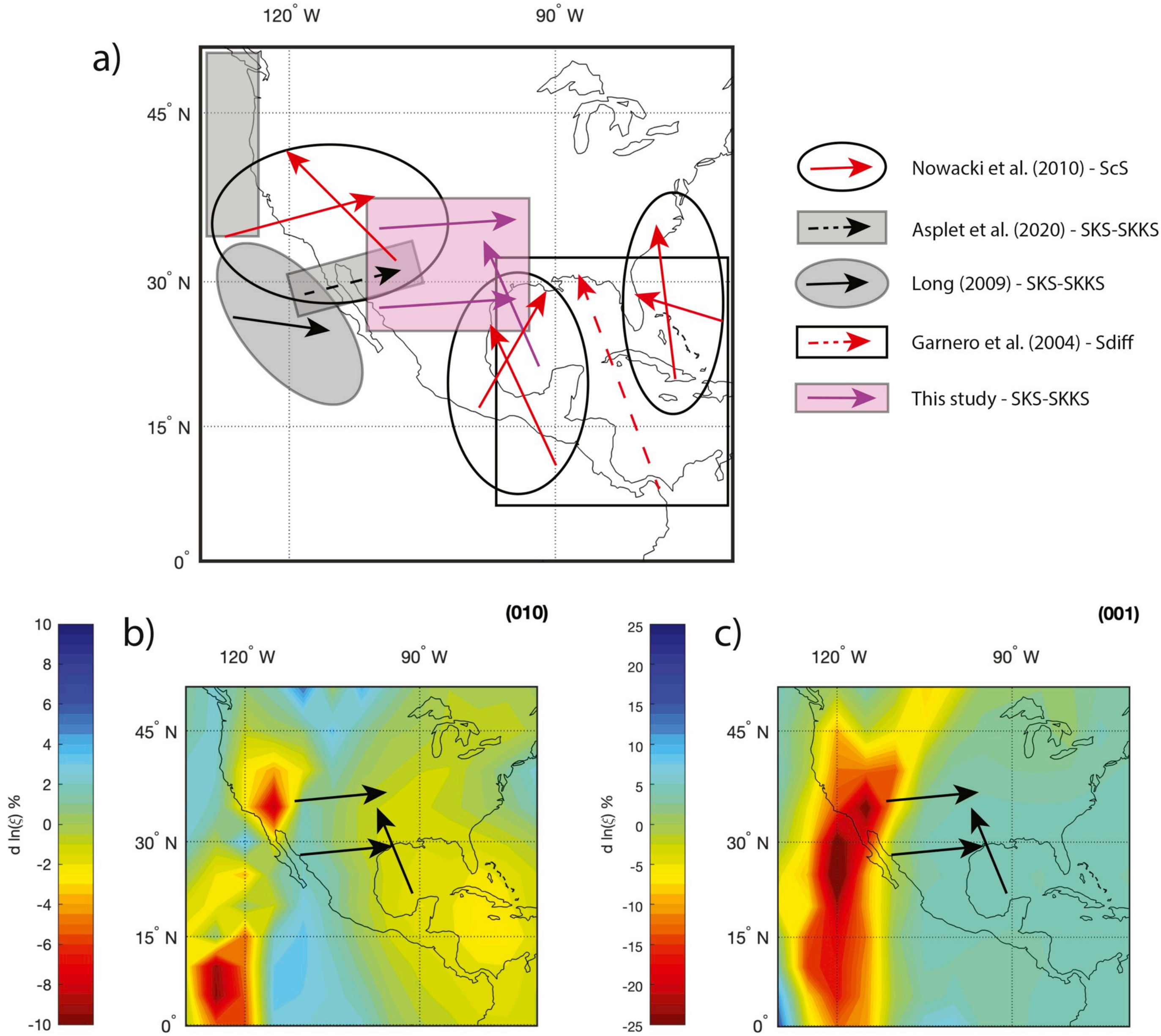

Fig. 7. a) View of lowermost mantle anisotropy beneath North America provided by our study and previous studies based on body waves. Map shows the approximate regions of inferred lowermost mantle anisotropy identified by Garnero et al. (2004) using S_{diff} phases, by Nowacki et al. (2010) using ScS phases, by Long (2009) and Asplet et al. (2020) using SKS-SKKS phases, and by our study, as shown in the legend. Arrows indicate the approximate raypaths used in each study. Note that the region offshore the U.S. Pacific Northwest identified by Asplet et al. (2020) extends substantially further to the west, beyond the limits of the map. b) Comparison between our measurements and the predictions of the Walker et al. (2011) flow and elasticity models. We plot predictions of radial anisotropy beneath North America from the work of Walker et al. (2011) for an elasticity model that invokes dominant slip on the (010) plane. c) Same as b), but for dominant slip on the (001) planes.

5. Discussion and modeling

5.1. Comparison with previous observations

Several previous studies have suggested the presence of anisotropy in the deepest mantle beneath North America and the surrounding region (Fig. 7). These include Garnero et al. (2004), who studied diffracted S waveforms that sampled the base of the mantle beneath the Caribbean and the Gulf of Mexico, just to the south and east of our study area, and Long (2009), who documented SKS-SKKS discrepancies due to lowermost mantle anisotropy beneath the eastern Pacific Ocean, just to the west of the region beneath the North American continent. More relevant for comparison here, Nowacki et al. (2010) studied anisotropy at the base of the mantle beneath North America by measuring the splitting of ScS phases. They found pervasive anisotropy in the lowermost mantle, including for a dense set of paths that sampled just to south and east of our study region, as well as for a few paths that sample just to the west of our discrepant SKS-SKKS pierce points. Based on their measurements, Nowacki et al. (2010) proposed that flow at the base of the mantle driven by a remnant of the Farallon slab results in the crystallographic alignment of post-perovskite; forward modeling showed that slip on the (010) plane provided the best fit to the data, although Nowacki et al. (2010, 2011) caution that this is based on a fairly rough, though plausible, idea of the likely mantle flow directions. A recently published study by Asplet et al. (2020) examined discrepant SKS-SKKS splitting for stations in the western and central U.S., applying a particularly careful analysis of errors and uncertainties in the characterization of discrepant pairs. Most of their data sampled well to the west of our study area, with good sampling beneath the eastern Pacific Ocean just to the north of the region studied by Long (2009). However, Asplet et al. (2020) document several discrepant pairs propagating along a west-to-east path whose sampling of the lowermost mantle partially overlaps with that of the discrepant pairs we document here, providing additional confirmation for our findings.

A careful comparison between our data set and that of Nowacki et al. (2010) reveals some interesting spatial correlations (Fig. 7). As mentioned above, the region of lowermost mantle anisotropy identified in our study is located just to the east of a region of anisotropy identified by Nowacki et al. (2010), although the latter study only has a few paths that sample the region (Fig. 7). Just to the south and east of our study region (beneath southern Mexico), Nowacki et al. (2010) identified splitting of ScS phases for a set of paths propagating to the northwest (Fig. 7), associated with earthquakes in South America and receivers in North America (with a few measurements for a crossing path). Interestingly, this region is sampled by a large number of SK(K)S phases propagating to the northeast in our study (Fig. 5), all of which are non-discrepant. The geographically extensive region beneath the central United States that was sampled only by non-discrepant pairs in our study (Fig. 5) was not examined by Nowacki et al. (2010) due to differences in raypath coverage. A third region of lowermost mantle anisotropy identified by Nowacki et al. (2010), centered just offshore of the southeastern U.S., was not sampled by our SKS-SKKS dataset. To summarize, we have found that one of the areas of lowermost mantle anisotropy identified by Nowacki et al. (2010) is geographically associated with SKS-SKKS splitting discrepancies in our study (or, more precisely, with a mix of discrepant and non-discrepant pairs), while another is associated with non-discrepant SKS-SKKS pairs.

We hypothesize that this difference reflects the details of the anisotropic geometry in each of the two regions, in combination with the raypath geometry used in each study. ScS phases, which were used in the Nowacki et al. (2010) study, propagate nearly horizontally through the lowermost mantle, while SK(K)S phases propagate at an oblique angle that is closer to vertical than horizontal. Recent modeling work (Creasy et al., 2019) has demonstrated the power of combining different types of data, including ScS and SKS-SKKS splitting, to constrain anisotropy at the base of the mantle, because they have different sensitivities to the anisotropic structure. We speculate that the anisotropy beneath central Mexico identified by Nowacki et al. (2010) using ScS splitting measurements is in a geometry that does not cause differential splitting of SKS and SKKS phases propagating to the northeast, because this set of paths shows no evidence for SKS-SKKS splitting discrepancies (Fig. 5). In contrast, the anisotropy beneath the southern U.S. and northern Mexico identified by Nowacki et al. (2010) from ScS splitting is likely in a geometry that causes discrepant splitting of SKS and SKKS phases in the geometry of our raypaths (Figs. 5 and 6).

5.2. Forward modeling

In order to further test the idea that anisotropy beneath North America is controlled by mantle flow driven by the remnants of the Farallon slab (Long, 2009; Nowacki et al., 2010; Asplet et al., 2020), we carried out some simple forward modeling of the region that exhibits SKS-SKKS splitting intensity discrepancies in our study based on previously published lowermost mantle elasticity scenarios. We did not carry out any modeling aimed at upper mantle anisotropy scenarios, because they have been thoroughly considered by other studies. For example, recent modeling studies by Lin et al. (2014) and Tesoniero et al. (2020) investigated the magnitude of SKS-SKKS discrepancies that arise from upper mantle anisotropy scenarios and showed that upper mantle anisotropy models yields generally small discrepancies in SKS-SKKS splitting intensities. We focus instead on modeling anisotropy geometries at the base of the mantle proposed by Walker et al. (2011), which take advantage of global flow models and simulations of texture development. Specifically, Walker et al. (2011) used a density structure inferred from Simmons et al. (2009) and a range of viscosity structures from Mitrovica and Forte (2004; viscosity profile V1 is tested here) to compute flow fields, and then predicted texturing in post-perovskite using a viscoplastic self-consistent (VPSC) approach (Lebensohn and Tomé, 1993) for a series of candidate dominant slip systems in post-perovskite. This model represents a quantitative prediction that is similar to the more qualitative idea of flow beneath North America proposed by Nowacki et al. (2010). Work by Nowacki et al. (2013) showed that the models of Walker et al. (2011) are broadly consistent with the ScS splitting observations of Nowacki et al. (2010) that reflect anisotropy at the base of the mantle beneath North America.

Our forward modeling approach relies on a ray theoretical approximation and follows previous work (Ford et al., 2015; Creasy et al., 2017; Reiss et al., 2019; Wolf et al., 2019). We extracted elastic tensors representing lowermost mantle anisotropy from the relevant portions of the global model of Walker et al. (2011) sampled by the SKS and SKKS phases in our dataset, for each of the two paths (west-east and south-north; Fig. 6). We tested all three of the possible dominant slip planes explored by Walker et al. (2011): (100), (010), and (001). For each candidate elastic tensor, we predicted the splitting of the relevant phase (SKS or SKKS) that is sampling the region, and then tested whether the predicted splitting parameters for the SKS-SKKS pairs were different enough to cause strongly discrepant splitting (as defined using the metrics in our data analysis and interpretation procedures). Splitting parameters were predicted using the MSAT package of Walker and Wookey (2012), which solves the Christoffel equation for a range of ray propagation directions. Our modeling approach is illustrated in Fig. 8, which shows the horizontal component of flow at the base of the mantle from Walker et al. (2011), along with visual representations of the splitting predicted from the relevant elastic tensors (for slip on the (010) plane, as an example) and the predicted splitting for SKS and SKKS phases for the ray propagation directions relevant for our study.

In addition to the traditional splitting parameters (ϕ, δt), we also predicted splitting intensity values, based on the known initial polarization directions of the SK(K)S phases (constrained to be equivalent to the backazimuth, given the P-to-S conversion at the CMB). Because we have not explicitly corrected our measurements for the effect of upper mantle anisotropy beneath the stations, the splitting intensity predictions are more relevant for our dataset. In contrast to the apparent splitting parameters (ϕ, δt), the splitting intensity is a commutative quantity (e.g., Silver and Long, 2011), and for the case of splitting due to multiple layers of anisotropy, it can be simply summed along the raypath. Because of this, the SKS-SKKS splitting intensity discrepancy should be independent of the upper mantle contribution to splitting intensity (assuming that it is the same for SKS and SKKS). Therefore, we can compare our modeled splitting intensity discrepancies to our observed ones, despite the fact that we have not carried out corrections for the upper mantle anisotropy. In contrast, a straightforward comparison between observed and modeled splitting parameters (ϕ, δt) cannot be carried out.

Results from our modeling for the Walker et al. (2011) elasticity scenarios based on dominant slip on the (010) and (001) planes are shown in Figs. 8 and 9, respectively. The (100) plane is thought to be a less likely candidate, but we have also computed predicted splitting for this model. Fig. 10 summarizes our full suite of modeling results. We show the differences in predicted splitting parameters for SKS and SKKS phases, both west-east and south-north paths, for each of the three elasticity models, including fast direction, delay time, and splitting intensity. For each type of measurement, we have marked on the plot the cutoff value for discrepancies that should be observable given the typical level of noise and size of error estimates (see Creasy et al. (2017, 2019) and Reiss et al. (2019) for further details). As demonstrated in Fig. 10, the Walker et al. (2011) models predict discrepancies in SKS-SKKS splitting for both propagation paths for all three elasticity

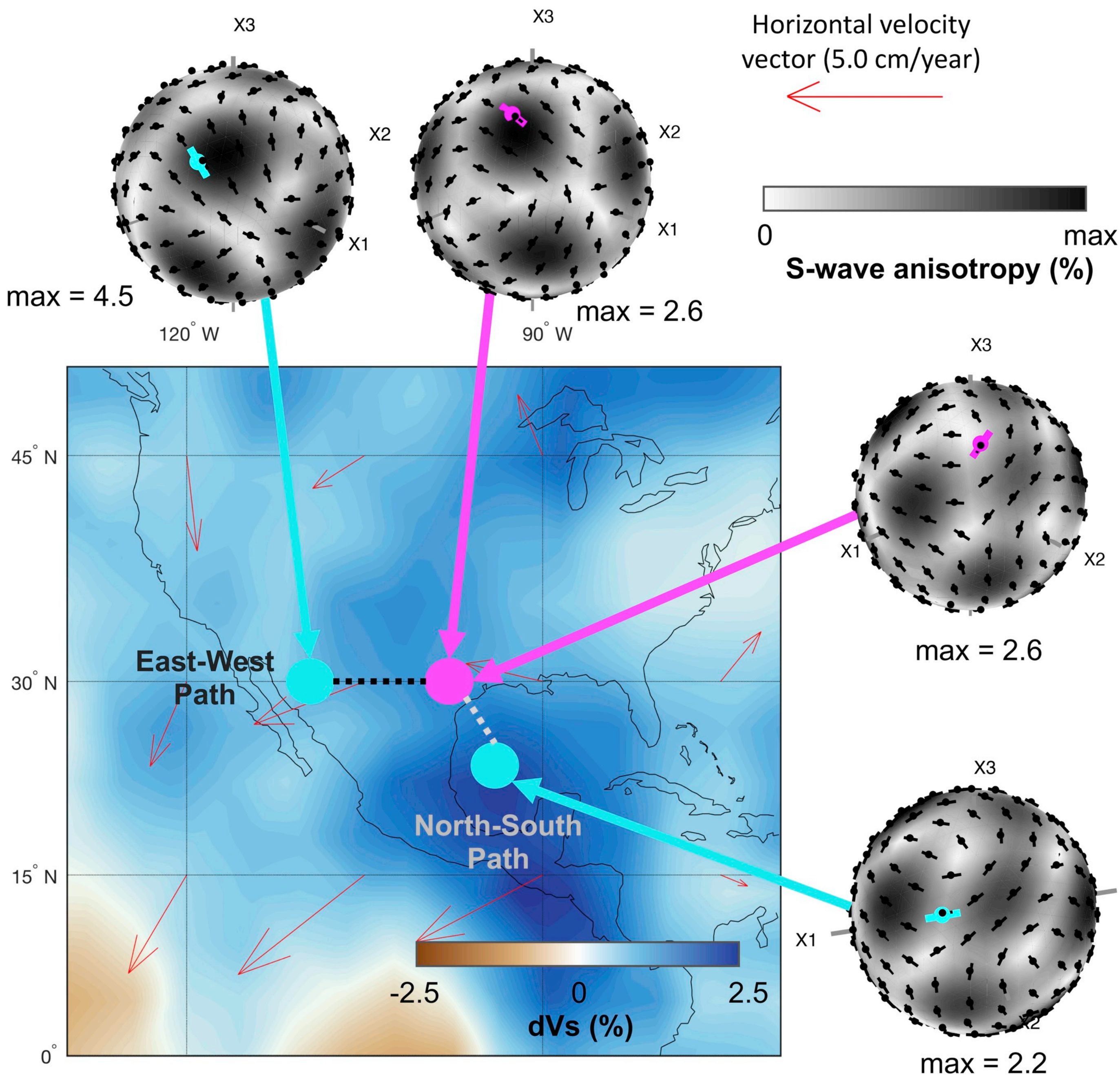

Fig. 8. Predicted splitting parameters for SKS and SKKS phases for the discrepant raypaths contained in our data set for the model of Walker et al. (2011), assuming dominant slip on the (010) plane in post-perovskite. Walker et al. (2011) used the TX2008V1 viscosity model to generate predictions for mantle flow and texture. Map view (lower left) shows the approximate average pierce points at a depth of 2700 km for the SKS phases (magenta) and for the SKKS phases (blue) for the east-west paths (dashed black line connecting the pierce points) and the north-south paths (dashed gray line). Background colors show shear velocities at the base of the mantle from the GyPSuM tomography model (Simmons et al., 2010), as indicated by the color bar. Red arrows show the horizontal component of predicted flow 150 km above the core-mantle boundary from the flow model used in Walker et al. (2011). For each pierce point, we show a 3D projection of predicted S-wave anisotropy, with gray scale representing the strength of anisotropy. For each plot, the maximum S-wave anisotropy (in %, corresponding to dark colors) is identified. Black lines on each plot represent predicted fast splitting directions over a range of ray propagation directions. The predicted fast splitting direction for the ray propagation corresponding to the phase of interest is shown in color (blue for SKKS, magenta for SKS). The X1, X2, and X3 axes correspond with geographic directions (north, west, and vertical, respectively). (For interpretation of the references to color in this figure legend, the reader is referred to the web version of this article.)

scenarios. Focusing on the splitting intensity predictions (bottom panel on Fig. 10), each of the models predicts some degree of splitting intensity discrepancy for both paths, consistent with our observations. For the (010) model, the magnitude of splitting intensity discrepancies is predicted to be modest (roughly 0.5 s for the west-east path and 1.5 s for the south-north path), while other models predict larger splitting intensity discrepancies. The relatively modest values of the intensity discrepancies predicted for the (010) model are most consistent with our results, and we note that Nowacki et al. (2010) favored slip on the (010) plane as most consistent with their ScS splitting results; however, all three elasticity scenarios from Walker et al. (2011) would predict splitting intensity discrepancies for our raypaths.

Another way of visualizing our results in the context of the Walker et al. (2011) flow and elasticity models is to examine the predictions of Walker et al. (2011) in map view. Fig. 7 shows the predicted anisotropy at the base of the mantle from Walker et al. (2011), for the same

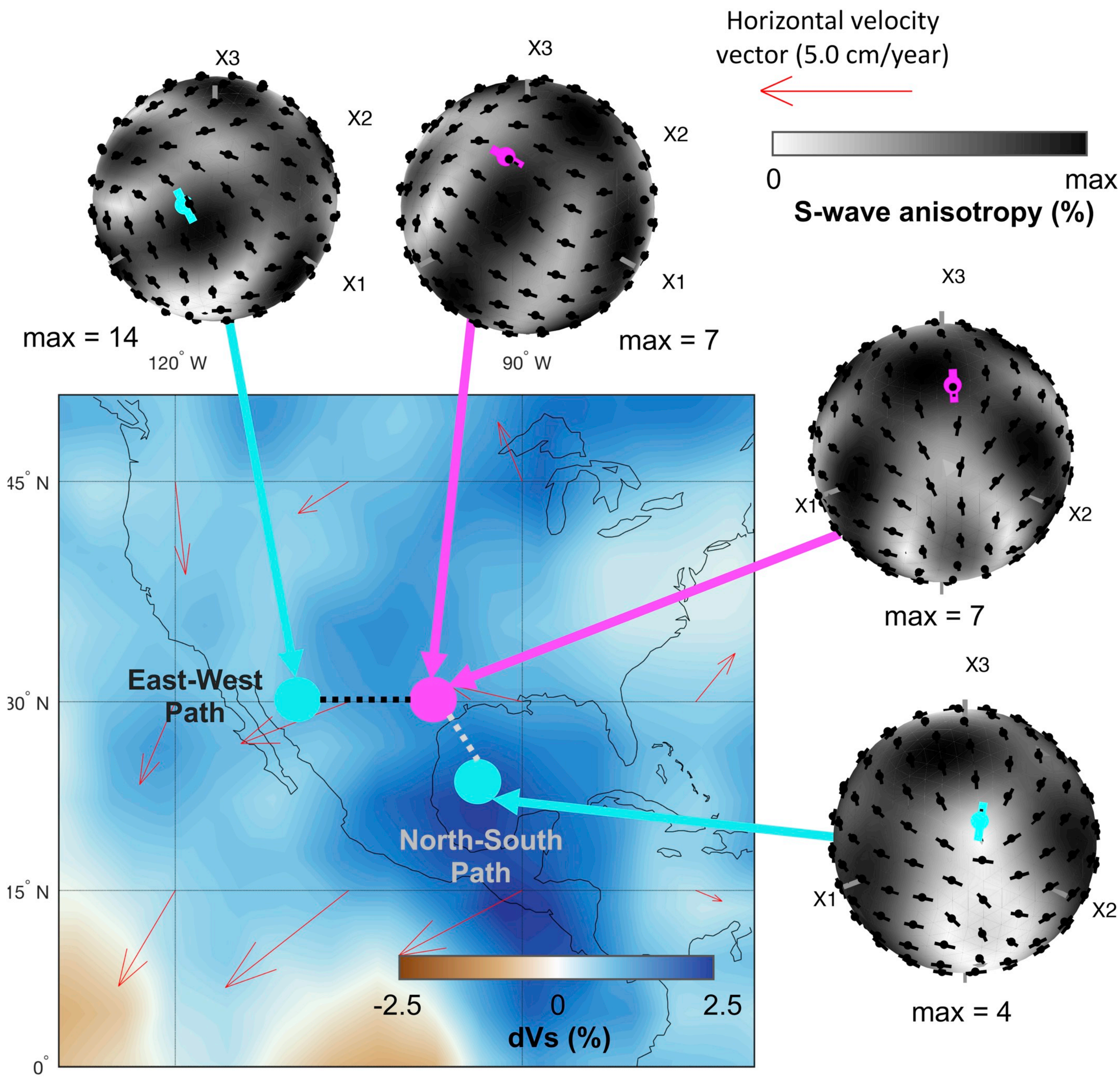

Fig. 9. Same as Fig. 8, except the elasticity model from Walker et al. (2011) that assumes dominant slip on the (001) plane is used. Plotting conventions are as in Fig. 7.

viscosity and flow model that was used to generate the predictions shown in Figs. 8–10. We show the predictions for the (001) and (010) dominant slip planes, as dominant slip on the (100) plane is thought to be less likely. Fig. 7 also shows in map view the regions of inferred lowermost mantle anisotropy that have been sampled by previous studies (Garnero et al., 2004; Long, 2009; Nowacki et al., 2010; Asplet et al., 2020). Following Walker et al. (2011), we plot perturbations to the radial anisotropy parameter, d ln(ξ) (in percent), where $\xi = (V_{SH})^2/(V_{SV})^2$, and we indicate on the map which regions our discrepant SKS-SKKS pairs are sampling. The Walker et al. (2011) models are dominated by flow driven by the remnant Farallon slab above the core-mantle boundary, which drives a region of upwelling (and thus strong negative perturbations to radial anisotropy) in a region extending from beneath Southern California to the south beneath the eastern Pacific Ocean, particularly for the (001) slip plane model. Interestingly, our discrepant SKS-SKKS measurements that propagate from west to east seem to sample the edge of this region of anomalous radial anisotropy, although the phases propagating from south to north do not.

We emphasize that while our simple modeling exercise has shown that our measurements are generally consistent with the models of Walker et al. (2011), in which lowermost mantle flow beneath North America is driven by downgoing Farallon slab remnants, our models are not unique. Other elasticity models likely exist that would also predict SKS-SKKS splitting discrepancies for the paths in our data set, including models that invoke other mechanisms for anisotropy, such as textured bridgmanite or ferropericlase (e.g., Nowacki et al., 2011; Creasy et al., 2019) or shape preferred orientation of partial melt or other elastically distinct material. Future modeling studies of lowermost mantle anisotropy beneath North America that not only take into account the full range of body wave observations (ScS splitting as well as the SKS-SKKS

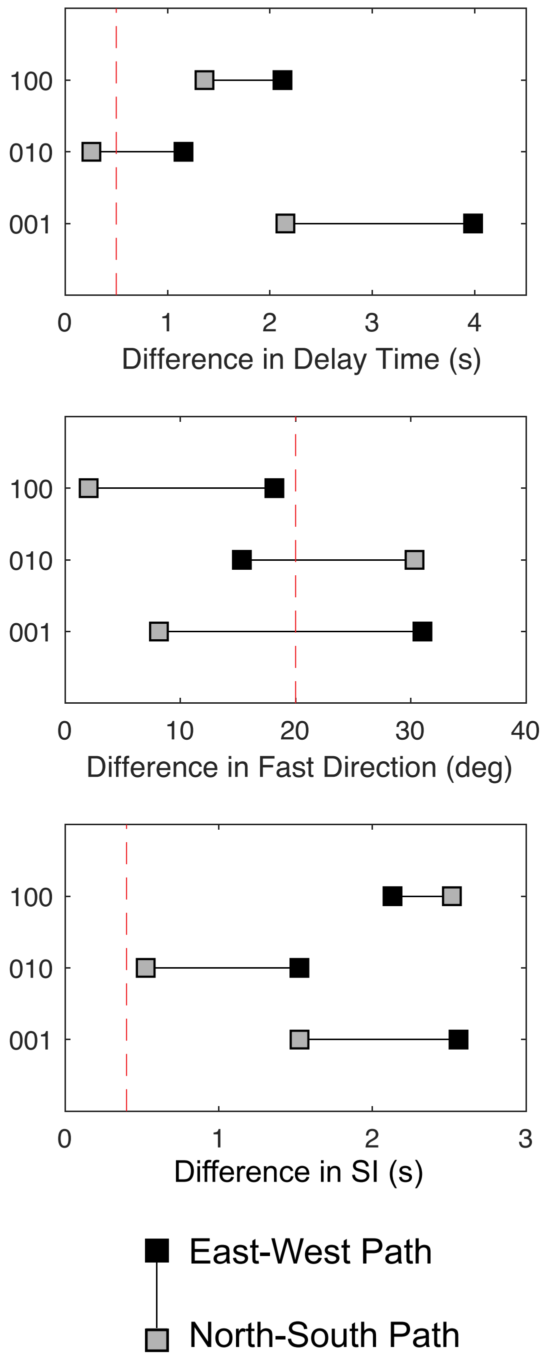

Fig. 10. Predictions of differences in shear wave splitting parameters for the SKS and SKKS phases in our dataset, based on the lowermost mantle elasticity model of Walker et al. (2011). We show the differences in predicted shear wave splitting delay times (top), in predicted fast splitting directions (middle), and in predicted splitting intensity (bottom). For each type of measurement, we show predictions for each of three possible dominant slip planes: (100), (010) (shown in Fig. 7), and (001) (shown in Fig. 8), as indicated. The predicted differences are shown for both the east-west ray propagation path in our data set (black squares) and for the north-south path (gray squares). On each plot, the vertical dashed red line indicates the typical cutoff value below which discrepancies between the SKS and SKKS phases would not be observed in real data (representing a difference in delay time of 0.5 s, a difference in fast direction of 20°, and a difference in splitting intensity of 0.4 s, respectively). The range of splitting intensity differences for discrepant pairs observed in our data is 0.4–0.8 s. Differences in fast directions and delay times are difficult to interpret in a straightforward way for our measurements because we did not explicitly correct for upper mantle contributions. (For interpretation of the references to color in this figure legend, the reader is referred to the web version of this article.)

discrepancies documented here) but also address a complete suite of possible mechanisms for anisotropy are needed. Furthermore, more sophisticated modeling tools that simulate global wave propagation and thus take into account finite-frequency effects (e.g., Nowacki and Wookey, 2016; Tesoniero et al., 2020), rather than relying on ray theory as in our study, should be applied in future work.

Finally, it would be useful for future modeling studies to explicitly grapple with whether the models of Walker et al. (2011), which predict some seismic anisotropy in the lowermost mantle throughout the sub-North America region, can be reconciled with our finding that most SKS-SKKS pairs in our dataset do not exhibit splitting discrepancies. There are several plausible explanations for this finding. As discussed in Section 4.2, a measurement of non-discrepant SKS-SKKS splitting does not necessarily imply an isotropic lower mantle, so it may be that these can be reconciled in a straightforward way. However, given the fact that beneath much of central North America, our data set exhibits non-discrepant pairs over a range of propagation directions, it is plausible that the structure of the lowermost mantle there is isotropic or only weakly anisotropic. It may be that there are significant lateral variations in the strength of anisotropy in the lowermost mantle beneath North America, such that there is relatively weak anisotropy (which causes only minor discrepancies in SKS-SKKS splitting) in most regions, with a local region of stronger anisotropy (which causes observable discrepancies in SKS-SKKS splitting) that is reflected in our measurements. Alternatively, it may be the case that very small-scale variations in lowermost mantle anisotropy beneath much of North America (on length scales smaller than those predicted by the Walker et al. (2011) models) exist and preclude a coherent contribution to the splitting of SK(K)S phases. Yet another possibility is that the lowermost mantle beneath North America makes isolated contributions to splitting, but generally such that the contributions to SKS and SKKS phases are similar. In any case, more detailed forward modeling studies of lowermost mantle anisotropy beneath North America that explore these questions more fully are warranted in the future.

5.3. Geodynamic implications

What do our SKS-SKKS splitting intensity discrepancy results imply about the structure and dynamics of the lowermost mantle beneath North America? First, it is notable that we identified discrepancies for a portion of the lowermost mantle that is adjacent to a fast velocity anomaly, thought to correspond to a remnant of the subducted Farallon slab at depth. This is consistent with the notion that particularly large strains, with deformation in the dislocation creep regime, may be induced at the base of the mantle when slabs impinge upon the CMB (McNamara et al., 2002). Furthermore, it is consistent with SKS-SKKS discrepancies observed at the edges of fast anomalies in the lowermost mantle in other regions, notably by Long (2009), Long and Lynner (2015), and Grund and Ritter (2018). It is striking, however, that we identified discrepant SKS-SKKS pairs only for a particular portion of the large fast velocity anomaly that extends beneath much of North America (Fig. 5).

We have carried out a qualitative comparison between our results, which suggest a region of anomalous anisotropy beneath the south-central U.S. and northern Mexico, and the predictions of flow patterns beneath North America from global models of mantle flow. As discussed previously, many of the discrepant SKS-SKKS paths documented in this study sample the eastern edge of a region of strong radial anisotropy predicted by a subset of the Walker et al. (2011) models (Fig. 7). In the global flow calculations that underpin the Walker et al. (2011) texture and anisotropy models, this feature is a consequence of a local region of upwelling flow. The presence of the Farallon slab further to the east (as evidenced by the fast velocity anomaly visible in our Fig. 5), which is impinging upon the CMB and driving downwelling, apparently drives flow to the west beneath the south-central U.S. (Fig. 7). Because our forward modeling (Section 5.2) predicts SKS-SKKS splitting intensity discrepancies for this scenario (Fig. 10), consistent with our observations, our study provides some support for this flow geometry (although we caution, again, that our models are not unique). We have also considered the global flow models of Flament (2019), which are based on constraints derived from plate reconstructions. Interestingly, the model of Flament (2019) predicts a pattern of upwelling and downwellings beneath North America that are similar to those in the Walker et al. (2011) model, although the horizontal flow direction in the region of the model associated with our SKS-SKKS splitting discrepancies is generally to the east, in contrast to the westward flow predicted by the models of Walker et al. (2011). Our region of discrepant SKS-SKKS splitting corresponds geographically to a region of transition from flow with a slight upwelling component to flow with a slight downwelling component in the Flament (2019) model. Because Flament (2019) did not predict texturing and anisotropy in the lowermost mantle, only a qualitative comparison between his model and our results is possible at this time, although more detailed quantitative modeling represents an obvious avenue for future work.

On the observational side, future work that extends our investigation of SKS-SKKS splitting discrepancies at a subset of USArray TA stations to the full TA network, and therefore includes good geographical coverage over a large backazimuthal range throughout the sub-North American lower mantle, will be necessary to confirm whether SKS-SKKS discrepancies are truly absent elsewhere beneath North America. In any case, however, our identification of a region of anomalous lowermost mantle anisotropy beneath the southern U.S. and northern Mexico, adjacent to a fast velocity anomaly and consistent with predictions derived from the global flow models of Walker et al. (2011), confirms previous suggestions that slab-driven flow in the lowermost mantle beneath North America produces observable seismic anisotropy (Long, 2009; Nowacki et al., 2010, 2013; Asplet et al., 2020), at least in certain regions.

6. Summary

We have examined waveforms of core-refracted shear waves measured at stations in North America for evidence of discrepant splitting behavior between pairs of SKS and SKKS phases. Using data from 269 stations located in eastern, southeastern, and western North America, we identified 279 high-quality pairs of SKS-SKKS waveforms. Of these, a small minority (15) exhibited SKS-SKKS splitting discrepancies that were strong enough to suggest a contribution to splitting of one or both phases from lowermost mantle anisotropy. The discrepant pairs sample a region of the lowermost mantle beneath the southern U.S. and northern Mexico, coincident with an isotropic fast velocity anomaly, in a region where lowermost mantle anisotropy has previously been inferred using a different type of observation. Given the character of SKS-SKKS splitting behavior documented in this study, we find no evidence that lowermost mantle anisotropy makes the primary contribution to SK(K)S splitting patterns at the stations we examined, and therefore it is appropriate to interpret them primarily in terms of upper mantle anisotropy. We carried out simple forward modeling to evaluate whether our observations are consistent with the previously proposed models of Walker et al. (2011) for lowermost mantle elasticity beneath North America and found that predictions of SKS-SKKS splitting intensity discrepancies based on these models are consistent with our observations. The measurements documented in this study are thus generally consistent with a geodynamic scenario in which remnants of the Farallon slab at the base of the mantle drive mantle flow. Additional work is needed to understand what controls the lateral variability in lowermost mantle anisotropy strength and/or geometry beneath North America that is suggested by the observations presented in this study.

Supplementary data to this article can be found online at https://doi.org/10.1016/j.pepi.2020.106504.

CRediT authorship contribution statement

Katherine A. Lutz:Formal analysis, Investigation, Visualization, Methodology, Writing - original draft.**Maureen D. Long**: Conceptualization, Funding acquisition, Methodology, Project administration, Supervision, Writing - original draft.**Neala Creasy**: Methodology, Software, Visualization, Writing - review & editing.**Jie Deng**:Methodology, Software, Visualization, Writing - review & editing.

Declaration of competing interest

The authors declare that they have no known competing financial interests or personal relationships that could have appeared to influence the work reported in this paper.

Acknowledgements

Seismic data from the U.S. National Seismic Network (doi:https://doi.org/10.7914/SN/US), the USArray Transportable Array (doi:https://doi.org/10.7914/SN/TA), the New England Seismic Network (doi:https://doi.org/10.7914/SN/NE), the Global Seismographic Network (doi:https://doi.org/10.7914/SN/IU), the Lamont-Doherty Cooperative Seismographic Network (network code LD), and the Intermountain West Seismic Network (doi:https://doi.org/10.7914/SN/IW) were used in this study. All data were accessed via the Data Management Center (DMC) of the Incorporated Research Institutions for Seismology (IRIS). IRIS Data Services are funded through the Seismological Facilities for the Advancement of Geoscience and EarthScope (SAGE) Proposal of the National Science Foundation (NSF) under Cooperative Agreement EAR-1261681. Some figures were prepared using the Generic Mapping Tools (Wessel and Smith, 1991). This work built on an initial pilot study by Xinxin Xu as part of a senior essay at Yale University (Xu, 2015). This study was funded via NSF grant EAR-1547499 to M.D.L. and via the Science, Technology, and Research Scholars (STARS) summer research program at Yale University. We are grateful to two anonymous reviewers for thorough, constructive, and insightful reviews that helped us to improve the paper.

References

Ando, M., Ishikawa, Y., Yamazaki, F., 1983. Shear wave polarization anisotropy in the upper mantle beneath Honshu, Japan. J. Geophys. Res. 88, 5850–5864.

Aragon, J.C., Long, M.D., Benoit, M.H., 2017. Lateral variations in SKS splitting across the MAGIC array, central Appalachians. Geochem. Geophys. Geosyst. 18, 4136–4155. https://doi.org/10.1029/2017GC007169.

Asplet, J., Wookey, J., Kendall, M., 2020. A potential post-perovskite province in D″ beneath the Eastern Pacific: evidence from new analysis of discrepant SKS-SKKS shear-wave splitting. Geophys. J. Int., ggaa114. https://doi.org/10.1093/gji/ggaa114.

Becker, T.W., Lebedev, S., Long, M.D., 2012. On the relationship between azimuthal anisotropy from shear wave splitting and surface wave tomography. J. Geophys. Res. 117, B01306. https://doi.org/10.1029/2011JB008705.

Chang, S.-J., Ferreira, A.M.G., Faccenda, M., 2016. Upper- and mid-mantle interaction between the Samoan plume and the Tonga-Kermadec slabs. Nat. Commun. 7, 10799. https://doi.org/10.1038/ncomms10799.

Chevrot, S., 2000. Multichannel analysis of shear wave splitting. J. Geophys. Res. 105, 21 579–21 590.

Cordier, P., Amodeo, J., Carrez, P., 2012. Modelling the rheology of MgO under Earth's mantle pressure, temperature and strain rates. Nature 481, 177–180. https://doi.org/10.1038/nature10687.

Cottaar, S., Romanowicz, B., 2013. Observations of changing anisotropy across the southern margin of the African LLSVP. Geophys. J. Int. 195 (2), 1184–1195. https://doi.org/10.1093/gji/ggt285.

Creasy, N., Long, M.D., Ford, H.A., 2017. Deformation in the lowermost mantle beneath Australia from observations and models of seismic anisotropy. J. Geophys. Res. 122, 5243–5267.

Creasy, N., Pisconti, A., Long, M.D., Thomas, C., Wookey, J., 2019. Constraining lowermost mantle anisotropy with body waves: a synthetic modelling study. Geophys. J. Int. 217, 766–783. https://doi.org/10.1093/gji/ggz049.

Creasy, N., Miyagi, L., Long, M.D., 2020. A library of elastic tensors for lowermost mantle

seismic anisotropy studies and comparison with seismic observations. Geochem. Geophys. Geosyst. 21, e2019GC008883. https://doi.org/10.1029/2019GC008883.
Crotwell, H.P., Owens, T.J., Ritsema, J., 1999. The TauP toolkit: flexible seismic travel-time and ray-path utilities. Seismol. Res. Lett. 70, 154–160.
Deng, J., Long, M.D., Creasy, N., Wagner, L., Beck, S., Zandt, G., Tavera, H., Minaya, E., 2017. Lowermost mantle anisotropy near the eastern edge of the Pacific LLSVP: constraints from SKS–SKKS splitting intensity measurements. Geophys. J. Int. 210, 774–786.
Flament, N., 2019. Present-day dynamic topography and lower-mantle structure from palaeogeographically constrained mantle flow models. Geophys. J. Int. 216, 2158–2182.
Ford, H.A., Long, M.D., He, X., Lynner, C., 2015. Lowermost mantle flow at the eastern edge of the African Large Low Shear Velocity Province. Earth Planet. Sci. Lett. 420, 12–22.
Garnero, E.J., McNamara, A.K., 2008. Structure and dynamics of the Earth's lower mantle. Science 320, 626–628.
Garnero, E.J., Revenaugh, J.S., Williams, Q., Lay, T., Kellogg, L.H., 1998. Ultralow velocity zone at the core–mantle boundary. In: Gurnis, M., Wysession, M., Knittle, E., Buffet, B. (Eds.), The Core–Mantle Boundary. American Geophysical Union, Washington, DC, pp. 319–334.
Garnero, E.J., Maupin, V., Lay, T., Fouch, M.J., 2004. Variable azimuthal anisotropy in Earth's lowermost mantle. Science 306, 259–262.
Garnero, E.J., McNamara, A.K., Shim, S.H., 2016. Continent-sized anomalous zones with low seismic velocity at the base of Earth's mantle. Nat. Geosci. 9, 481–489.
Grund, M., Ritter, J.R.R., 2018. Widespread seismic anisotropy in Earth's lowermost mantle beneath the Atlantic and Siberia. Geology 47, 123–126.
He, X., Long, M.D., 2011. Lowermost mantle anisotropy beneath the northwestern Pacific: evidence from PcS, ScS, SKS, and SKKS phases. Geochem. Geophys. Geosyst. 12, Q12012. https://doi.org/10.1029/2011GC003779.
Hernlund, J.W., Thomas, C., Tackley, P.J., 2005. A doubling of the post-perovskite phase boundary and structure of the Earth's lowermost mantle. Nature 434, 882–886.
Karato, S.I., Jung, H., Katayama, I., Skemer, P., 2008. Geodynamic significance of seismic anisotropy of the upper mantle: new insights from laboratory studies. Annu. Rev. Earth Planet. Sci. 36, 59–95.
Kraych, A., Carrez, P., Cordier, P., 2016. On dislocation glide in $MgSiO_3$ bridgmanite at high-pressure and high-temperature, Earth Planet. Sci. Lett. 452, 60–68.
Kennett, B.L.N., Engdahl, E.R., Buland, R., 1995. Constraints on seismic velocities in the Earth from traveltimes. Geophys. J. Int. 122, 108–124. https://doi.org/10.1111/j.1365-246X.1995.tb03540.x.
Lebensohn, R.A., Tomé, C.N., 1993. A self-consistent anisotropic approach for the simulation of plastic deformation and texture development of polycrystals: application to zirconium alloys. Acta Metall. Mater. 41, 2611–2624.
Li, Y., Levin, V., Elkington, S., Hlavaty, J., 2019. Localized anisotropic domains beneath eastern North America. Geochem. Geophys. Geosyst. 20, 5499–5521. https://doi.org/10.1029/2019GC008518.
Lin, Y.-P., Zhao, L., Hung, S.-H., 2014. Full-wave effects on shear wave splitting. Geophys. Res. Lett. 41, 799–804.
Long, M.D., 2009. Complex anisotropy in D″ beneath the eastern Pacific from SKS-SKKS splitting discrepancies, Earth Planet. Sci. Lett. 285, 181–189.
Long, M.D., 2013. Constraints on subduction geodynamics from seismic anisotropy. Rev. Geophys. 51, 76–112. https://doi.org/10.1002/rog.20008.
Long, M.D., Lynner, C., 2015. Seismic anisotropy in the lowermost mantle near the Perm Anomaly. Geophys. Res. Lett. 42, 7073–7080.
Long, M.D., Benoit, M.H., Chapman, M.C., King, S.D., 2010. Upper mantle anisotropy and transition zone thickness beneath southeastern North America and implications for mantle dynamics. Geochem. Geophys. Geosyst. 11, Q10012. https://doi.org/10.1029/2010GC003247.
Long, M.D., Jackson, K.G., McNamara, J.F., 2016. SKS splitting beneath Transportable Array stations in eastern North America and the signature of past lithospheric deformation. Geochem. Geophys. Geosyst. 17, 2–15. https://doi.org/10.1002/2015GC006088.
Long, M.D., Silver, P.G., 2009. Shear wave splitting and mantle anisotropy: Measurements, interpretations, and new directions. Surv. Geophys. 30, 407–461. https://doi.org/10.1007/s10712-009-9075-1.
Lynner, C., Long, M.D., 2012. Evaluating contributions to SK(K)S splitting from lower mantle anisotropy: a case study from station DBIC, Côte D'Ivoire. Bull. Seism. Soc. Am. 102, 1030–1040. https://doi.org/10.1785/0120110255.
Lynner, C., Long, M.D., 2014. Lowermost mantle anisotropy and deformation along the boundary of the African LLSVP. Geophys. Res. Lett. 41, 3447–3454. https://doi.org/10.1002/2014GL059875.
Lynner, C., Long, M.D., 2015. Heterogeneous seismic anisotropy in the transition zone and uppermost lower mantle: evidence from South America, Izu-Bonin and Japan. Geophys. J. Int. 201, 1545–1552. https://doi.org/10.1093/gji/ggv099.
Marquardt, H., Miyagi, L., 2015. Slab stagnation in the shallow lower mantle linked to an increase in mantle viscosity. Nat. Geosci. 8, 311–314.
McNamara, A.K., 2019. A review of large low shear velocity provinces and ultra low velocity zones. Tectonophysics 760, 199–220.
McNamara, A.K., van Keken, P.E., Karato, S., 2002. Development of anisotropic structure by solid-state convection in the Earth's lower mantle. Nature 416, 310–314.
Mitrovica, J.X., Forte, A.M., 2004. A new inference of mantle viscosity based upon joint inversion of convection and glacial isostatic adjustment data, Earth Planet. Sci. Lett. 225, 177–189. https://doi.org/10.1016/j.epsl.2004.06.005.
Mohiuddin, A., Long, M.D., Lynner, C., 2015. Mid-mantle seismic anisotropy beneath southwestern Pacific subduction systems and implications for mid-mantle deformation. Phys. Earth Planet. Inter. 245, 1–14.
Monteiller, V., Chevrot, S., 2010. How to make robust splitting measurements for single-station analysis and three-dimensional imaging of seismic anisotropy. Geophys. J. Int. 182, 311–328.
Murakami, M., Hirose, K., Kawamura, K., Sata, N., Ohishi, Y., 2004. Post-perovskite phase transition in MgSiO3. Science 304, 855–858.
Niu, F., Perez, A.M., 2004. Seismic anisotropy in the lower mantle: A comparison of waveform splitting of SKS and SKKS. Geophys. Res. Lett. 31, L24612. https://doi.org/10.1029/2004GL021196.
Nowacki, A., Wookey, J., 2016. The limits of ray theory when measuring shear wave splitting in the lowermost mantle with ScS waves. Geophys. J. Int. 207, 1573–1583. https://doi.org/10.1093/gji/ggw358.
Nowacki, A., Wookey, J., Kendall, J.M., 2010. Deformation of the lowermost mantle from seismic anisotropy. Nature 467, 1091–1094.
Nowacki, A., Wookey, J., Kendall, J.M., 2011. New advances in using seismic anisotropy, mineral physics and geodynamics to understand deformation in the lowermost mantle. J. Geodyn. 52, 205–228.
Nowacki, A., Walker, A.M., Wookey, J., Kendall, J.-M., 2013. Evaluating post-perovskite as a cause of D″ anisotropy in regions of palaeosubduction. Geophys. J. Int. 192, 1085–1090. https://doi.org/10.1093/gji/ggs068.
Nowacki, A., Kendall, J.M., Wookey, J., Pemberton, A., 2015. Mid-mantle anisotropy in subduction zones and deep water transport. Geochem. Geophys. Geosyst. 16, 764–784. https://doi.org/10.1002/2014GC005667.
Panning, M., Romanowicz, B., 2006. A three-dimensional radially anisotropic model of shear velocity in the whole mantle. Geophys. J. Int. 167, 361–379.
Pisconti, A., Thomas, C., Wookey, J., 2019. Discriminating between causes of D″ anisotropy using reflections and splitting measurements for a single path. J. Geophys. Res. Solid Earth 124, 4811–4830. https://doi.org/10.1029/2018JB016993.
Reiss, M.C., Long, M.D., Creasy, N., 2019. Lowermost mantle anisotropy beneath Africa from differential splitting of SKS-SKKS phases. J. Geophys. Res. 124. https://doi.org/10.1029/2018JB017160.
Restivo, A., Hellfrich, G., 2006. Core-mantle boundary structure investigated using SKS and SKKS polarization anomalies. Geophys. J. Int. 165, 288–302.
Romanowicz, B., Wenk, H.R., 2017. Anisotropy in the deep earth. Phys. Earth Planet. Inter. 269, 58–90.
Roy, S.K., Kumar, M.R., Srinagesh, D., 2014. Upper and lower mantle anisotropy inferred from comprehensive SKS and SKKS splitting measurements from India, Earth Planet Sci. Lett. 392, 192–206. https://doi.org/10.1016/j.epsl.2014.02.012.
Silver, P.G., Chan, W.W., 1988. Implications for continental structure and evolution from seismic anisotropy. Nature 335, 34–39.
Silver, P.G., Long, M.D., 2011. The non-commutivity of shear wave splitting operators at low frequencies and implications for anisotropy tomography. Geophys. J. Int. 184, 1415–1427. https://doi.org/10.1111/j.1365-246X.2010.04927.x.
Simmons, N.A., Forte, A.M., Grand, S.P., 2009. Joint seismic, geodynamic and mineral physics constraints on three-dimensional mantle heterogeneity: implications for the relative importance of thermal vs. compositional heterogeneity. Geophys. J. Int. 177, 1284–1304.
Simmons, N.A., Forte, A.M., Boschi, L., Grand, S.P., 2010. GyPSuM: a joint tomographic model of mantle density and seismic wave speeds. J. Geophys. Res. 115, B12310. https://doi.org/10.1029/2010JB007631.
Tesoniero, A., Leng, K., Long, M.D., Nissen-Meyer, T., 2020. Full wave sensitivity of SK(K)S phases to arbitrary anisotropy in the upper and lower mantle. Geophys. J. Int. 222, 412–435. https://doi.org/10.1093/gji/ggaa171.
Vinnik, L.P., Farra, V., Romanowicz, B., 1989. Azimuthal anisotropy in the earth from observations of SKS at GEOSCOPE and NARS broad-band stations. Bull. Seismol. Soc. Am. 79, 1542–1558.
Vinnik, L.P., Stunff, Y.L., Makeyeva, L., 1995. Seismic anisotropy in the D″ layer. Geophys. Rev. Lett. 22, 1657–1660.
Wagner, L.S., Long, M.D., Johnston, M.D., Benoit, M.H., 2012. Lithospheric and asthenospheric contributions to shear-wave splitting observations in the southeastern United States, Earth Planet Sci. Lett. 341, 128–138. https://doi.org/10.1016/j.epsl.2012.06.020.
Walker, A.M., Wookey, J., 2012. MSAT – a new toolkit for the analysis of elastic and seismic anisotropy. Comput. Geosci. 49, 81–90. https://doi.org/10.1016/j.cageo.2012.05.031.
Walker, A.M., Forte, A.M., Wookey, J., Nowacki, A., Kendall, J.-M., 2011. Elastic anisotropy of D″ predicted from global models of mantle flow. Geochem. Geophys. Geosyst. 12, Q10006. https://doi.org/10.1029/2011GC003732.
Walpole, J., Wookey, J., Masters, G., Kendall, J.M., 2014. A uniformly processed data set of SKS shear wave splitting measurements: a global investigation of upper mantle anisotropy beneath seismic stations. Geochem. Geophys. Geosyst. 15, 1991–2010. https://doi.org/10.1002/2014GC005278.
Wang, Y., Wen, L., 2007. Complex seismic anisotropy at the border of a very low velocity province at the base of the Earth's mantle. J. Geophys. Res. 112, B09305. https://doi.

org/10.1029/2006JB004719.
Wessel, P., Smith, W.H.F., 1991. Free software helps map and display data, Eos Trans. AGU 72, 441. https://doi.org/10.1029/90EO00319.
White-Gaynor, A.L., Nyblade, A.A., 2016. Shear wave splitting across the Mid-Atlantic region of North America: a fossil anisotropy interpretation. Geology 45, 555–558. https://doi.org/10.1130/G38794.1.
Wolf, J., Creasy, N., Pisconti, A., Long, M.D., Thomas, C., 2019. An investigation of seismic anisotropy in the lowermost mantle beneath Iceland. Geophys. J. Int. 219, S152–S166.
Wookey, J., Kendall, J.M., Rumpker, G., 2005a. Lowermost mantle anisotropy beneath the North Pacific from differential S-ScS splitting. Geophys. J. Int. 161, 829–838.
Wookey, J., Stackhouse, S., Kendall, J.M., Brodholt, J., Price, G., 2005b. Efficacy of the post-perovskite phase as an explanation for lowermost mantle seismic properties. Nature 438, 1004–1007.
Wüstefeld, A., Bokelmann, G., Barruol, G., Zaroli, C., 2008. Splitlab: A shear-wave splitting environment in Matlab. Comput. Geosci. 34, 515–528.
Xu, X., 2015. Seismic Anisotropy in the Lower Mantle underneath North America from SKS-SKKS Splitting Discrepancies. Yale University, B.S. thesis.
Yang, B.B., Liu, Y., Dahm, H., Liu, K.H., Gao, S.S., 2017. Seismic azimuthal anisotropy beneath the eastern United States and its geodynamic implications. Geophys. Res. Lett. 44, 2670–2678. https://doi.org/10.1002/2016GL071227.
Yuan, K., Beghein, C., 2014. Three-dimensional variations in Love and Rayleigh wave azimuthal anisotropy for the upper 800 km of the mantle. J. Geophys. Res. Solid Earth 119 (4), 3232–3255.